Conditional moment method for fully coupled phase-averaged cavitation models

Spencer H. Bryngelson[a,*], Franz O'Meally[b], Tim Colonius[a], Rodney O. Fox[c,d]

[a] Division of Engineering and Applied Science, California Institute of Technology, Pasadena, CA 91125, USA
[b] Department of Mechanical Engineering, Johns Hopkins University, Baltimore, MD 21218, USA
[c] Department of Chemical and Biological Engineering, Iowa State University, Ames, IA 50011, USA
[d] Center for Multiphase Flow Research and Education, Iowa State University, Ames, IA 50011, USA

Abstract

Eulerian sub-grid models for the bubble dynamics associated with cavitation are an increasingly viable route for simulating engineering-scale bubbly flow problems. We identify two primary concerns towards enabling physically faithful simulations: sub-grid model fidelity and computational cost. Previous Euler–Euler models considered the sub-grid bubble radius R and radial velocity $\dot{R}$ to be deterministic functions of the bubble dynamics model and pressure forcing. We relax this assumption, allowing R and $\dot{R}$ to be arbitrary probability density functions conditioned on the equilibrium bubble size R_o. Conditional moment inversion methods reconstruct quadrature nodes and weights in the internal coordinate directions, which are then used to compute the moments that close the fully coupled flow equations. A one-dimensional acoustically excited bubble screen is used to study the resulting models. Computationally, resolving R and $\dot{R}$ variations requires only a modest additional cost when compared to that of the R_o-coordinate, which has a highly oscillatory behavior. The observed bubble screen pressures show that variation of the bubble probability density functions lead to variations in the dynamic response of the bubble screen. For example, we observe an increase in pressure fluctuations with increasing R variation, as the bubbles oscillate at shorter time scales than the transmitted acoustic wave, while increasing $\dot{R}$ variation reduces the observed pressure fluctuations. Thus, modeling the R–$\dot{R}$ distributions is necessary if actual cavitating bubble clouds are in such statistical disequilibria.

Keywords: Quadrature moment methods, bubbly flow, cavitation, sub-grid model, phase averaging

1. Introduction

Cavitation and the resulting bubble cloud dynamics are of broad engineering interest. Examples include blast trauma [1], kidney stone pulverization lithotripsy [2], and flows over ship propellers and hydrofoils [3]. Direct simulation of bubble dynamics and interaction with acoustic waves is largely precluded due to spatial and temporal scale separation: small bubbles nucleate and oscillate rapidly relative to the larger and longer features of suspending flow.

Sub-grid methods can address these flows via ensemble phase averaging (Euler–Euler) or local volume averaging (Euler–Lagrange). Our previous review of phase averaging showed that Euler–Euler averaging methods can enable simulation of engineering-scale cavitating flows [4]. However, these models must pay special attention to the polydispersity associated with the bubbles. For example, actual bubble clouds are distributed in their equilibrium bubble size R_o [5, 6]. When this distribution is broad, this leads to considerable dispersion and ultimately damping of the average response of the bubbles to pressure fluctuations [7, 8]. Previous studies assumed deterministic bubble dynamic

*Corresponding author; spencer@caltech.edu

Preprint submitted to the 11th International Symposium on Cavitation

independent variables, e.g. the bubble radii R and their radial velocities $\dot{R}$. This is appropriate for transient flows starting from rest (since all bubbles start in equilibrium), but in flows past immersed bodies, bubbles nucleated upstream are not necessarily in a state of equilibrium. Thus, in general, sub-grid bubble models should consider the bubble state to be stochastic and associated with an evolving probability distribution function.

To understand the relative importance of these evolving density functions, we use a fully coupled conditional quadrature moment method to assess the bubble dynamic behavior and computational cost in the face of non-deterministic bubble state. This method can describe the evolving bubble dynamics statistics, even as skewness and kurtosis form at large pressure ratios [9]. Specifically, our method uses the conditional hyperbolic quadrature method of moments (CHyQMOM) [10], which does not *a priori* assume a static distribution shape. Our implementation couples CHyQMOM to the compressible flow equations as in Bryngelson et al. [4]. Section 2 details this formulation and the bubble model that closes it.

As a first step toward analyzing the behavior of these models in relevant flows, we consider an acoustically excited bubble screen [11]. The subsequent bubble dynamics are a function of the initial number density functions. We vary the breadth of initially log-normal and normal profiles for radial and radial velocity coordinates, respectively, and observe how the resulting bubble dynamics (and radiated pressure fluctuations) are altered. Section 3 details the ability of our method to represent the evolving statistics of fully polydisperse bubble dynamics, and section 4 provides concluding remarks.

2. Phase-averaging model formulation

2.1. Flow equations

Our formulation of the ensemble-averaged equations follows that of Zhang and Prosperetti [12] and Ando [13]. A complete description of them is included in previous works [4]. In brief, they differentiate from the multi-component compressible flow equations via modifications to the liquid pressure and volume fraction equations. These modifications include functions of the evolving bubble statistics that are computed via quadrature rules as discussed next.

2.2. Quadrature moment method

The statistics evolve dynamically according to a population balance equation (PBE) for the number density function $f(\boldsymbol{\xi})$, which represents the bubble dynamics in terms of its internal coordinates $\boldsymbol{\xi} = \{R, \dot{R}, R_o\}$, where R is the bubble radius, $\dot{R}$ is its time derivative, and R_o is the equilibrium bubble radius. Following a usual procedure [14], we describe f via a finite set of raw moments μ_{lmn} where l, m, and n correspond to the R, $\dot{R}$, and R_o coordinate directions. The moment transport equations follow from [9]:

$$\frac{\partial \mu_{lmn}}{\partial t} = l\mu_{l-1,m+1,n} + m\int_{\Omega} \ddot{R}(\boldsymbol{\xi}) R^l \dot{R}^{m-1} R_o^n f(\boldsymbol{\xi})\, \mathrm{d}\boldsymbol{\xi}. \tag{1}$$

Since R_o is not a dynamic variable, the total moments are recast as

$$\mu_{lmn} = \int_{\Omega_{R_o}} f(R_o) R_o^m \mu_{lm}(R_o)\, \mathrm{d}R_o \quad \text{where} \quad \mu_{lm}(R_o) = \int_{\Omega_{R\times\dot{R}}} f(R,\dot{R}|R_o) R^l \dot{R}^m\, \mathrm{d}R\mathrm{d}\dot{R} \tag{2}$$

Here, $f(R_o)$ is a static log-normal distribution corresponding to polydispersity and $f(R,\dot{R}|R_o)$ are the conditional number density functions. Since $f(R_o)$ is time stationary, the first integral is computed with a fixed quadrature formula. Conditional moment methods approximate the multi-dimensional moments $\mu_{lm}(R_o)$ [15, 16]. The right-hand-side of (1) is closed via a bubble dynamics model for $\ddot{R}$, which is discussed next.

2.3. Bubble dynamic model

As a first step towards more realistic sub-grid modeling, we consider the bubbles as spherical and gas-filled with dynamics governed by a Rayleigh–Plesset equation:

$$R\ddot{R} + \frac{3}{2}\dot{R}^2 + \frac{4}{\mathrm{Re}}\frac{\dot{R}}{R} = \left(\frac{R_o}{R}\right)^{3\gamma} - \frac{1}{C_p(t)}. \tag{3}$$

In (3), Re is the Reynolds number (dimensionless ratio of inertial to viscous effects) and $C_p(t) \equiv p_l(t)/p_0$ is the ratio of suspending liquid and atmospheric pressures. The bubble contents compress via a polytropic adiabatic process with coefficient $\gamma = 1.4$. Hereon, all quantities are non-dimensionalized by the liquid density, ambient pressure, and equilibrium bubble size. In future implementations, this model can be supplanted by a more complex one that more faithfully represents the bubble dynamics and cavitation physics.

3. Results

3.1. Uncoupled bubble dynamics statistics in the R–$\dot{R}$ phase-space

We first assess the ability of CHyQMOM to represent the statistics of bubbles that are R_o-monodisperse but display R and $\dot{R}$ variation. Log-normal and normal distributions initialize the statistics, with variances σ_R^2 and $\sigma_{\dot{R}}^2$ for the R and $\dot{R}$ dynamics, respectively. The bubbles respond to constant and uniform pressure forcing C_p.

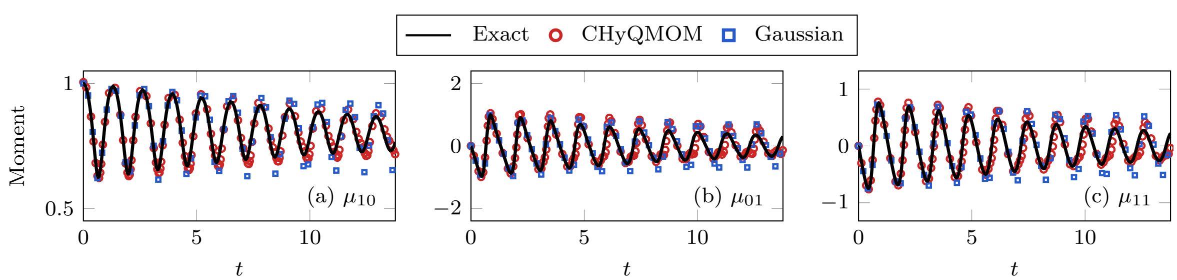

Figure 1: Example moments as labeled for bubbles with $R_o = 1$ and $\mathrm{Re} = 10^2$ and dimensionless shape parameters $\sigma_R = \sigma_{\dot{R}} = 0.2$. The CHyQMOM implementation uses two quadrature nodes in each internal coordinate direction and Gaussian corresponds to Gaussian closure [4]. Monte Carlo simulations with 10^4 provides the surrogate exact solution.

Figure 1 shows the evolution of an example moment set for forcing $C_p = 0.3$, though the conclusions drawn from this moment set and pressure ratio represent a broad range of C_p and higher-order moments alike. The shape parameters σ_R is chosen to be of similar size as σ_{R_o} for sea water (≈ 0.7 [17]) The figure shows that the 4-node CHyQMOM closure is sufficient to represent the moments. The discrete L_2 error for up to second-order moments are smaller for CHyQMOM than Gaussian closure (see [9]). Thus, we move forward with 4-node CHyQMOM for its accuracy and low cost.

3.2. *Fully coupled polydisperse bubble screens*

We next assess the bubble dynamics and statistics in an acoustically excited dilute screen region. The bubble screen parameterization generally matches that of Bryngelson et al. [4], with a width of 5 mm and initial void fraction $\alpha_o = 10^{-4}$. The acoustic wave is a single period of a sinusoid with peak amplitude $0.3 p_0$ and frequency 300 kHz. MFC, our open-source flow solver, solves the governing equations with a fifth-order-accurate diffuse interface method and third-order-accurate SSP–RK3 time integration [18].

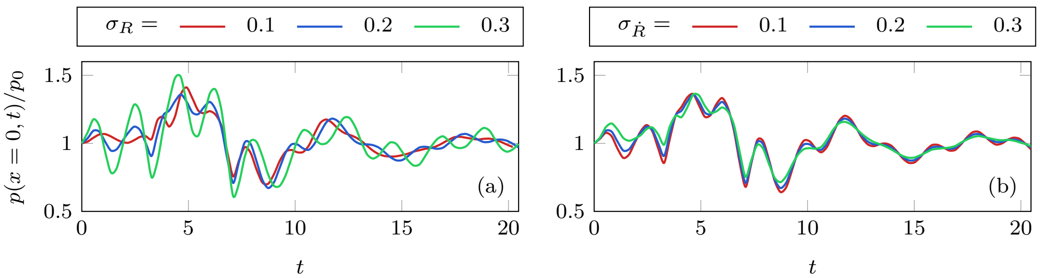

Figure 2: Bubble-screen-centered pressure before, during, and after excitement due to an acoustic wave. The bubbles are polydisperse with log-normal R_o distribution ($\sigma_{R_o} = 0.2$) and $\mathrm{Re} = 10^3$. Panels (a) and (b) show variation in σ_R and $\sigma_{\dot{R}}$, respectively, about a $\sigma_R = \sigma_{\dot{R}} = 0.2$ representative state.

Figure 2 shows the dynamics associated with a bubble screen in varying degrees of statistical disequilibrium. Panel (a) shows a shorter-wavelength oscillatory behavior superimposing the longer acoustic waves. These oscillations are larger in amplitude for larger σ_R. Panel (b) shows that phase-cancellation smooths the pressure profile, with increasingly smooth profiles for larger $\sigma_{\dot{R}}$. Together, behaviors are qualitatively similar to those associated with varying R_o distribution widths. Thus, tuning an R_o distribution based upon single-probe pressure measurements may be insufficient.

In the results of figure 2, Simpson's rule with 61 nodes closes the moment system in the R_o internal coordinate, Thus, resolving R_o-polydispersity, not R–$\dot{R}$ statistics, is the the primary computational cost of the simulations. As a result, analyzing the effect of R and $\dot{R}$ variation on more complex cavitating flows should not be prohibitive.

4. Conclusion

We introduced a fully coupled numerical method for simulating sub-grid cavitating bubble dispersions with a full representation of the evolving bubble statistics. Our results showed that only four quadrature points are required to represent the statistics of the bubble dynamic variables when the population has one equilibrium radius. Modeling for this variation results in a qualitatively different pressure response of an excited bubble screen. Thus, modeling the R–$\dot{R}$ distributions is necessary if actual bubble clouds are in such statistical disequilibria; validation of this will be the subject of future work. Our results also show that phase-cancellation can modestly reduce some computational costs associated with resolving the R_o coordinate. However, R_o-direction quadrature costs still dominate the solution of broadly polydisperse bubble populations. This leaves the door open to novel approaches for reducing the computational cost of R_o-polydispersity.

Acknowledgements

This work was supported by the US Office of Naval Research under grant numbers N0014-17-1-2676 and N0014-18-1-2625.

References

[1] K. Laksari, S. Assari, B. Seibold, K. Sadeghipour, K. Darvish, Computational simulation of the mechanical response of brain tissue under blast loading, Biomech. Model. Mechanobiol. 14 (2015) 459–472.

[2] K. Maeda, T. Colonius, Bubble cloud dynamics in an ultrasound field, J. Fluid Mech. 862 (2019) 1105–1134.

[3] P. A. Chang, M. Ebert, Y. L. Young, Z. Liu, K. Mahesh, H. Jang, M. Shearer, Propeller forces and structural response due to crashback, in: 27th Symposium on Naval Hydrodynamics, 2008.

[4] S. H. Bryngelson, K. Schmidmayer, T. Colonius, A quantitative comparison of phase-averaged models for bubbly, cavitating flows, Int. J. Mult. Flow 115 (2019) 137–143.

[5] M. Vanni, Approximate population balance equations for aggregation breakage processes, J. Colloid Interface Sci. 221 (2000) 143–160.

[6] K. Ando, T. Colonius, C. E. Brennen, Numerical simulation of shock propagation in a polydisperse bubbly liquid, Int. J. Mult. Flow 37 (2011) 596–608.

[7] P. Smereka, A Vlasov equation for pressure wave propagation in bubbly fluids, J. Fluid Mech. 454 (2002) 287–325.

[8] T. Colonius, R. Hagmeijer, K. Ando, C. E. Brennen, Statistical equilibrium of bubble oscillations in dilute bubbly flows, Phys. Fluids 20 (2008).

[9] S. H. Bryngelson, A. Charalampopoulos, T. P. Sapsis, T. Colonius, A Gaussian moment method and its augmentation via LSTM recurrent neural networks for the statistics of cavitating bubble populations, Int. J. Multiph. Flow 127 (2020) 103262.

[10] R. O. Fox, F. Laurent, A. Vié, Conditional hyperbolic quadrature method of moments for kinetic equations, J. Comput. Phys. 365 (2018) 269–293.

[11] S. N. Domenico, Acoustic wave propagation in air-bubble curtains in water–Part I: History and theory, Geophysics 47 (1982) 345–353.

[12] D. Z. Zhang, A. Prosperetti, Ensemble phase-averaged equations for bubbly flows, Phys. Fluids 6 (1994).

[13] K. Ando, Effects of polydispersity in bubbly flows, Ph.D. thesis, California Institute of Technology, 2010.

[14] R. O. Fox, Computational models for turbulent reacting flows, Cambridge University Press, 2003.

[15] C. Yuan, R. O. Fox, Conditional quadrature method of moments for kinetic equations, J. Comput. Phys. 230 (2011) 8216–8246.

[16] R. G. Patel, O. Desjardins, R. O. Fox, Three-dimensional conditional hyperbolic quadrature method of moments, J. Comp. Phys. X 1 (2019) 100006.

[17] T. J. O'Hern, L. D'Agostino, A. J. Acosta, Comparison of holographic and coulter counter measurements of cavitation nuclei in the ocean, J. Fluids Eng. 110 (1988) 200–207.

[18] S. H. Bryngelson, K. Schmidmayer, V. Coralic, J. C. Meng, K. Maeda, T. Colonius, MFC: An open-source high-order multi-component, multi-phase, and multi-scale compressible flow solver, Comp. Phys. Comm. (2020) 107396.